Sensor placement for structural damage identification by means of topology optimization

Bartłomiej Błachowski, **Mariusz Ostrowski, Piotr Tauzowski, Andrzej** Świercz, **and** Łukasz **Jankowski**

View Online   Export Citation

ARTICLES YOU MAY BE INTERESTED IN

The types of derivatives and bifurcation in fractional mechanics
AIP Conference Proceedings **2239**, 020001 (2020); https://doi.org/10.1063/5.0007796

Energy harvesting of a composite beam with optimizing stacking sequence of layers
AIP Conference Proceedings **2239**, 020003 (2020); https://doi.org/10.1063/5.0007788

Vibration of plates partially and totally immersed in fluid by the boundary element method
AIP Conference Proceedings **2239**, 020017 (2020); https://doi.org/10.1063/5.0007819

Sensor placement for structural damage identification by means of topology optimization

Bartłomiej Błachowski[a)], Mariusz Ostrowski[b)], Piotr Tauzowski[c)],
Andrzej Świercz[d)] and Łukasz Jankowski[e)]

Institute of Fundamental Technological Research, Polish Academy of Sciences
Pawińskiego 5B, 02-106 Warsaw, Poland.

[a)]Corresponding author: bblach@ippt.pan.pl
[b)] mostr@ippt.pan.pl , [c)] ptauzow@ippt.pan.pl , [d)] aswiercz@ippt.pan.pl , [e)] ljank@ippt.pan.pl

Abstract. The success of virtually all structural health monitoring (SHM) methods depends on the information content of the measurements, and thus on the placement of the available sensors. This paper presents an efficient method for finding optimal sensor distribution over structural system with many degrees of freedom (DOFs). The objective function is based on the classical Fisher information matrix. Originally, this yields a computationally hard discrete optimization problem. However, the proposed numerical solution method is based on a concept taken from structural topology optimization, where a discrete optimization problem is replaced with a continuous one. Two numerical examples demonstrate the effectiveness of the proposed methodology. These are a 5-bay truss with 24 DOFs and a two-story frame structure whose finite element model has been condensed to 14 DOFs.

INTRODUCTION

Damage identification attracted a lot of attention during the last three decades [1-5]. The reason is the fact that large number of existing civil infrastructures reached their service life and growing number of structures is equipped with Structural Health Monitoring (SHM) systems. A successful structural damage identification is determined by three inseparably coupled factors: sensor placement, damage location and its extent, and finally location and time-frequency characteristics of the applied excitation [6,7].

The purpose of this study is to address the first of the mentioned aspects, namely optimal sensor placement. A vast literature has been devoted to optimal sensor placement methods, and a very recent example is an approach based on the Virtual Distortion Method and described in [8]. The Effective Independence (EI) method proposed by Kammer [9] is one of the most successfully applied in practice. However, the EI method is dedicated rather to test-analysis correlation and therefore more specific methods for damage identification are still needed. Additionally, in the case of large civil structures, which are intended to be equipped with large amount of sensors of different types, other sensor placement methods can be more efficient. Recently, a promising idea of utilizing a topology optimization approach for the purpose of sensor placement has been proposed by Bruggi and Mariani [10]. The goal of this study is to extend their method, which has been verified on a plate structure, to the case of finite element (FE) models of truss and frame structures that consist multi degrees of freedom.

The main purpose of this work is to find the optimal arrangement of sensors on the structure to detect defects most accurately. The objective function for the problem formulated in this way is the total weighted difference between the deformation of a damaged and undamaged state. This problem is very similar to the topological optimization, where one searches for the optimal material distribution minimizing the mass of the structure while meeting the conditions related to some mechanical properties such as the maximum displacement of the structure, stress intensity or load capacity [11]. This similarity suggests that topological optimization can be applied to the problem of optimal

placement of damage locating sensors [12]. Two numerical examples presented in this study prove the applicability of topological optimization for the optimal sensor placement problem.

DISCRETE FORMULATION FOR THE SENSOR PLACEMENT OPTIMIZATION

Sensor placement is essentially a combinatorial problem, which can be expressed by the following well-known formula

$$\binom{N_d}{N_s} = \frac{N_d!}{N_s!(N_d-N_s)!}, \tag{1}$$

where N_d denotes the number of the candidate sensor locations and N_s represents the number of sensors to be distributed over all candidate locations. It will be shown in the next section dealing with numerical examples that even for relatively simple problems the number of combinations arising from eq. (1) can be very large and in general case the exact global optimum is not known. Before describing efficient methods for finding an approximate solution to the sensor placement problem some basic results from the estimation theory will be briefly recalled.

Estimation error and metrics for optimal sensor placement

In this section one of the most frequently used metrics for this problem is considered. The derivation of the formula for estimation error starts with the following observation equation:

$$\mathbf{y}(t) = \mathbf{\Phi}_s \mathbf{\eta}(t) + \mathbf{w}(t), \tag{2}$$

where $\mathbf{y} \in \mathbb{R}^{N_s}$, $\mathbf{\Phi}_s \in \mathbb{R}^{N_s \times N_m}$ and $\mathbf{w} \in \mathbb{R}^{N_s}$. The vector $\mathbf{y}$ contains the measurement data from sensors, $\mathbf{\Phi}_s$ is modal matrix obtained by choosing columns representing measured modes and rows corresponding to the degrees of freedom (DOFs) at which sensors are located. The vector $\mathbf{\eta}$ in eq. (2) contains modal coordinates of the measured modes, $\mathbf{w}$ is vector of measurement errors, N_s is number of sensors and N_m is number of measured modes. The vector $\mathbf{w}$ is assumed as stationary Gaussian white noise which is uncorrelated and has the expected value equal to zero. The noise is characterized by the variance σ^2 for each sensor.

Estimation of the modal coordinates $\mathbf{\eta}$ can be obtained by the least squares:

$$\hat{\mathbf{\eta}}(t) = \left(\mathbf{\Phi}_s^{\mathrm{T}} \mathbf{\Phi}_s\right)^{-1} \mathbf{\Phi}_s^{\mathrm{T}} \mathbf{y}(t). \tag{3}$$

Estimation error of the modal coordinates shown above is equal to $\mathbf{e}(t) = \hat{\mathbf{\eta}}(t) - \mathbf{\eta}(t)$. The covariance matrix $\mathbf{C}$ of the estimation error is given by the formula below

$$\mathbf{C} = \mathbb{E}\{\mathbf{e}(t)\mathbf{e}^{\mathrm{T}}(t)\} = \sigma^2 \left(\mathbf{\Phi}_s^{\mathrm{T}} \mathbf{\Phi}_s\right)^{-1}. \tag{4}$$

The operator $\mathbb{E}$ represents here the expected value operator. Estimator (3) is unbiased and efficient, so the covariance matrix $\mathbf{C}$ is equal to the inverse of the Fisher information matrix $\mathcal{F}$ [13]:

$$\mathbf{C} = \mathcal{F}^{-1}. \tag{5}$$

In this case the Fisher information matrix is expressed by the formula below

$$\mathcal{F} = \frac{1}{\sigma^2} \mathbf{\Phi}_s^{\mathrm{T}} \mathbf{\Phi}_s \tag{6}$$

If the variance σ^2 is the same for each sensor, the Fisher information matrix can be written in a simplified form:

$$\mathcal{F} = \mathbf{\Phi}_s^{\mathrm{T}} \mathbf{\Phi}_s. \tag{7}$$

From eq. (7) it follows that the norm of $\mathbf{C}$ can be minimized by maximization of the norm of $\mathcal{F}$. Three norms are frequently used in the literature [14]:
1. *A-optimality* - average-variance criterion, $\text{tr}(\mathbf{C})$.
2. *E-optimality* - largest-eigenvalue criterion, $\lambda_{\max}(\mathbf{C})$.
3. *D-optimality* - determinant criterion, $\ln \det(\mathbf{C})$.

Previously for finding the optimal sensor configurations the *A-optimality* was used, however recently some advantages of the *D-optimality* have been shown [15] and nowadays this norm is the most frequently applied in search for the optimal sensor arrangement. Determinant of $\mathcal{F}$ takes into account non-orthogonality of the vectors that appear in $\mathbf{\Phi}_S$ matrix. Thanks to this property motion of the structure in one of the identified modes disturbs less the measurement of other identified modes. In this study, the *D-optimality* norm is considered in further calculations.

Background information about the Effective Independence method

This subsection introduces the Reader into the famous Effective Independence (EI) method. The goal for recalling this basic information is that it will be helpful in comparison with the topology optimization based method described here. Derivations performed in this subsection will be used in the next subsection to show the convergence of the topology optimization based method.

The idea of the so-called Effective Independence has been introduced by Kammer in 1991 [9]. Based on this concept, he proposed an algorithm that allows an approximate solution to be found in iterative manner. His approach consists in removing in each iteration the i-th DOF from the set of the candidate sensor locations S_{all}, which has the least contribution to $\det(\mathcal{F})$. This method, in its essence, does not maximize the determinant of the Fisher information matrix $\mathcal{F}$ but provides the least decrease of the determinant during all iterations, when the rows of $\mathbf{\Phi}_S$ corresponding to the candidate sensors locations are removed.

Fisher information matrix is symmetric so its determinant can be calculated as the product of all eigenvalues:

$$\det(\mathcal{F}) = \prod_{k=1}^{N_m} \lambda_k. \tag{8}$$

From symmetry of $\mathcal{F}$ it follows also that

$$\mathbf{\Psi}^{\text{T}} \mathcal{F} \mathbf{\Psi} = \mathbf{\Lambda}, \tag{9}$$

where: $\mathbf{\Psi} = [\mathbf{\psi}_1 \quad \cdots \quad \mathbf{\psi}_k \quad \cdots \quad \mathbf{\psi}_{N_m}]$ is the matrix of the eigenvectors $\mathbf{\psi}_k$ that constitute an orthonormal basis ($\mathbf{\Psi}^{\text{T}}\mathbf{\Psi} = \mathbf{I}$) called by Kammer the absolute identification space, $\mathbf{\Lambda} = \text{diag}(\lambda_1, \dots \lambda_k, \dots \lambda_{N_m})$. Formula (10) follows from eq. (9).

$$\mathbf{E} = \underbrace{[\mathbf{\Phi}_S\mathbf{\Psi}] \circ [\mathbf{\Phi}_S\mathbf{\Psi}]}_{\mathbf{G}} \mathbf{\Lambda}^{-1} \tag{10}$$

Here $\circ$ is the Hadamard product (element by element). Each k-th column of the matrix $\mathbf{G}$ sums to λ_k, and in the matrix $\mathbf{E}$ to the unity, i.e., each column is normalized by the appropriate eigenvalue. Maximization of such a normalized sum is equivalent to maximization of the product in eq. (8). It is convenient to define the vector

$$\mathbf{e}_D = \left[\sum_{k=1}^{N_m} e_{1k} \quad \cdots \quad \sum_{k=1}^{N_m} e_{ik} \quad \cdots \quad \sum_{k=1}^{N_m} e_{N_s k}\right]^{\text{T}} \tag{11}$$

containing in each its i-th element e_{Di} participation of the i-th sensor in the effective independence along all identification directions $\mathbf{\psi}_k$, where e_{ik} is element of the matrix $\mathbf{E}$:

$$e_{ik} = \frac{(\mathbf{\phi}_{Si}\mathbf{\psi}_k)^2}{\lambda_k}. \tag{12}$$

Here $\mathbf{\phi}_{Si}$ is i-th row of the matrix $\mathbf{\Phi}_S$. From equations (9) and (10) it follows that vector $\mathbf{e}_D$ can be defined as the diagonal of matrix $\mathbf{E}_{\mathcal{F}}$:

$$\begin{aligned}
\mathbf{E}_{\mathcal{F}} &= \mathbf{\Phi}_S \mathbf{\Psi} \mathbf{\Lambda}^{-1} \mathbf{\Psi}^{\mathrm{T}} \mathbf{\Phi}_S{}^{\mathrm{T}} \\
&= \mathbf{\Phi}_S \mathcal{F}^{-1} \mathbf{\Phi}_S{}^{\mathrm{T}} \\
&= \mathbf{\Phi}_S \left(\mathbf{\Phi}_S{}^{\mathrm{T}} \mathbf{\Phi}_S \right)^{-1} \mathbf{\Phi}_S{}^{\mathrm{T}}.
\end{aligned} \tag{13}$$

The vector $\mathbf{e}_D = \mathrm{diag}(\mathbf{E}_{\mathcal{F}})$ serves for calculation of effective independence distribution. Algorithm proposed by Kammer in each iteration removes the row of $\mathbf{\Phi}_S$ that is related to the least element of $\mathbf{e}_D$ [16]. Then having the matrix $\mathbf{\Phi}_S$ reduced by one row, $\mathbf{e}_D$ is calculated once again using $\mathbf{E}_{\mathcal{F}}$ from equation (13) and the iteration is repeated for another row. Repeating of iterations is interrupted when the number of rows in $\mathbf{\Phi}_S$ is smaller than the number of the desired sensors or the rank of $\mathbf{E}_{\mathcal{F}}$ is smaller than the number of modes N_m.

The last line of eq. (13) shows that the matrix $\mathbf{E}_{\mathcal{F}}$ is idempotent, i.e. $\mathbf{E}_{\mathcal{F}}{}^2 = \mathbf{E}_{\mathcal{F}}$. The matrix $\mathbf{E}_{\mathcal{F}}$ is of rank N_m for each iteration while the matrix $\mathbf{\Phi}_S$ consists of N_m linearly independent columns. The matrix $\mathbf{E}_{\mathcal{F}}$, as each idempotent matrix, after a suitable transformation of coordinates (diagonalization) can be expressed in the form shown below:

$$\mathbf{L}^{-1} \mathbf{E}_{\mathcal{F}} \mathbf{L} = \begin{bmatrix} \mathbf{I}_{N_m \times N_m} & \mathbf{0}_{N_m \times N_r} \\ \mathbf{0}_{N_r \times N_m} & \mathbf{0}_{N_r \times N_r} \end{bmatrix} = \tilde{\mathbf{E}}_{\mathcal{F}}, \tag{14}$$

where: $\mathbf{L}$ is the transformation matrix consisting of the eigenvectors of $\mathbf{E}_{\mathcal{F}}$, $\mathbf{I}_{N_m \times N_m}$ is the identity matrix of rank N_m, $N_r = N_s - N_m$, and $\mathbf{0}._\times.$ are zero matrices of appropriate dimensions. From properties of the trace operator and transformation (14) it follows that the rank of any idempotent matrix is equal to its trace. Equation (14) tells that until $N_s = N_m$ there exist sensor locations which are not necessary to achieve the linear independence of the identified mode shapes. The dimensions of the matrices $\mathbf{E}_{\mathcal{F}}$ and $\tilde{\mathbf{E}}_{\mathcal{F}}$ decrease by one with each iteration of the algorithm. If during an iteration for any i-th DOF $e_{Di} = 1$, then the removal the i-th DOF causes a reduction of the identity matrix $\mathbf{I}_{N_m \times N_m}$ into $\mathbf{I}_{N_m-1 \times N_m-1}$ inside the matrix $\tilde{\mathbf{E}}_{\mathcal{F}}$ and a collapse of the linear independence. Removal of the DOF for which $e_{Di} < 1$ causes dimension reduction from matrices $\mathbf{0}_{N_r \times N_r}$, $\mathbf{0}_{N_r \times N_m}$ and $\mathbf{0}_{N_m \times N_r}$ to $\mathbf{0}_{N_r-1 \times N_r-1}$, $\mathbf{0}_{N_r-1 \times N_m}$ and $\mathbf{0}_{N_m \times N_r-1}$.

CONTINUOUS APPROACH BY MEANS OF THE PROPOSED TOPOLOGY OPTIMIZATION BASED METHOD

The proposed method transforms the combinatorial problem described in previous section into a continuous one [14]. The method is called topology optimization based because of its similarity to the topology optimization based methods used in structural optimization [11].

The proposed approach consists in providing the so called sensor density function. For a discretized structure, such a function is a vector

$$\mathbf{\rho} \in [0,1]^{N_d}. \tag{15}$$

Instead of an iterative removal of rows from $\mathbf{\Phi}_S$, each i-th row of the matrix $\mathbf{\Phi}$ is multiplied by the i-th element ρ_i of $\mathbf{\rho}$ related to the i-th DOF according to formula (16).

$$\mathbf{\Phi}_C = \mathrm{Diag}(\mathbf{\rho})\mathbf{\Phi}, \tag{16}$$

where $\mathrm{Diag}(\mathbf{\rho})$ is the diagonal matrix with $\mathbf{\rho}$ on the diagonal. In eq. (16), $\mathbf{\Phi}$ is the full available modal matrix, and $\mathbf{\Phi}_C$ has rows scaled by the sensor density function $\mathbf{\rho}$. The sensor density function $\mathbf{\rho}$ in the proposed method represents the distribution of the sensors throughout the structure, and it can be compared to the diagonal $\mathbf{e}_D$ of the idempotent matrix, which quantifies the participation of the individual sensors in the effective independence, see eq. (11).

Each iteration of the method consists of the two following main steps:
1. Update the values in the vector $\mathbf{\rho}$ while keeping it normalized as $\|\mathbf{\rho}\|_1 = m$.
2. Change the participation of rows in the determinant of the Fisher information matrix with the use of the sensor density function $\mathbf{\rho}$ (16).

In each iteration the elements of the vector $\mathbf{\rho}$ should change their values in such a way that some of them increase asymptotically to 1 when others decrease asymptotically to 0. Such a procedure reveals the sensors which have the largest contribution to the linear independence in the sense of the metric $\mathbf{e}_D$.

In the further part of this paper it will be shown that the proposed method always choses such a number of sensors that it is equal to the number N_m of modes selected for monitoring, except a special case of spatial symmetry of the FEM mesh. Numerical example of such a symmetry is shown in the further part of the paper. From this fact it follows that it is not possible to separate sensor placement into two different formulations, namely:

- Minimize the number of sensors subject to the permitted chosen norm of **C**.
- Minimize the chosen norm of variation **C** subject to the permitted number of sensors.

Proposed method imposes the following problem formulation:

> **maximize**   determinant of the Fisher Information Matrix,
> **subject to**:   number of sensors equal to number of identified modes.

If it is desired to have more sensors than the number of the identified modes, it is possible to impose a larger value of N_m.

At each iteration of the algorithm, the elements of the vector $\boldsymbol{\rho}$ are normalized similarly to the elements of $\mathbf{e}_D$ in eq. (11) by the eigenvalues of $\mathcal{F}$, see eq. (10). It follows that during the iterative process suitable elements of the vector $\boldsymbol{\rho}$ can increase only at the expense of the other ones. The matrix $\mathbf{E}_{\mathcal{F}}^{C}$ is also idempotent, but instead of changing its size at each iteration, like in Kammers's method, only the transformation matrices into the matrix $\tilde{\mathbf{E}}_{\mathcal{F}}$ introduced in equation (14) are changed. Here, the dimension of the matrix $\tilde{\mathbf{E}}_{\mathcal{F}}$ is the same for each iteration and equals $N_d \times N_d$.

ILLUSTRATIVE EXAMPLES

This section presents two illustrative examples. The first of them demonstrates a local behavior of the proposed algorithm. On a relatively simple example of a planar truss it is shown that the proposed method produces results similar to the Effective Independence method, but still cannot guarantee finding the global optimum. The second example in the form of a two-story frame structure demonstrates the effectiveness of the method and its fast convergence to the final solution.

Example 1: Five-bay truss structure

The first example concerns the five-bay truss structure shown in Figure 1. The structure is assumed to be made of steel elements with a length of $l_x=l_y=51$ cm having the cross section areas $A=10^{-4}$ m^2, mass density $\rho=7850$ kg/m^3 and Young's modulus $E=200$ GPa.
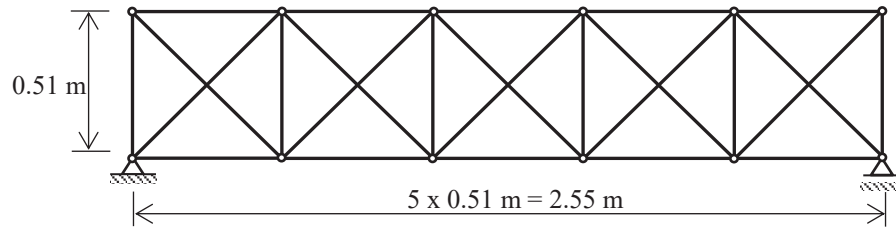

FIGURE 1. Five-bay truss structure

The task is to find the location for three sensors that the first three modes to be optimally monitored. These mode shapes and the corresponding natural frequencies are shown in Figure 2a-c). The sensors are equally allowed to measured vertical or horizontal displacement. The node numbering is presented in Figure 3. The following formulas have been used to identify the number of the degrees of freedom corresponding to the individual nodes: $i_{d,x} = 2i_n - 1$ and $i_{d,y} = 2i_n$ for horizontal and vertical directions, respectively. Based on these formulas, one can easily find that node no. 1 has assigned DOF no. 1 and 2, node no. 2 DOF no. 3 and 4 and so on.
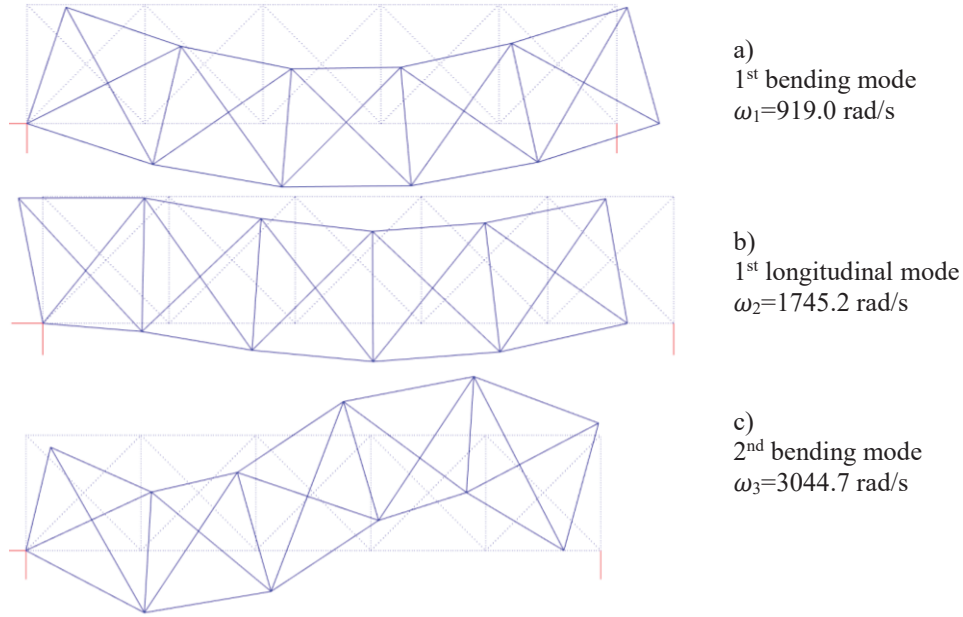
a)
1st bending mode
ω_1=919.0 rad/s

b)
1st longitudinal mode
ω_2=1745.2 rad/s

c)
2nd bending mode
ω_3=3044.7 rad/s

FIGURE 2. First three mode shapes of the analyzed truss
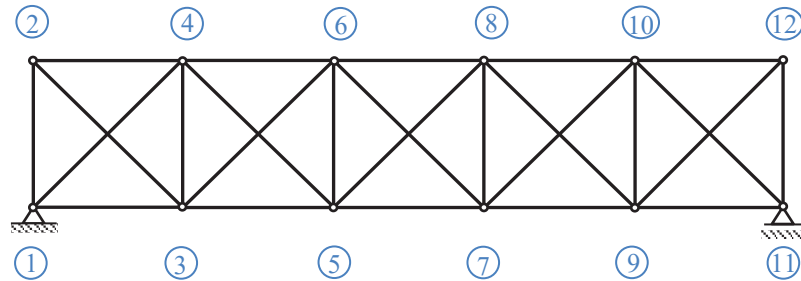

FIGURE 3. Node numbering in the analyzed truss

From Figure 3 it is also evident that in this example there were 24 DOFs and all of them were used as candidate locations ($N_d = 24$). As it was mentioned earlier, the goal is to find the optimal location of 3 sensors for identification of the modal amplitudes of the first three modes ($N_s = 3$). Substituting these numbers into eq. (1), as many as 2024 possible configurations for sensor location are obtained.

TABLE 1. Comparison of the optimal solution obtained by different methods

Optimization method	No. of measured degree of freedom	Value of FIM determinant
Effective independence	10, 18, 21	2.0491
Proposed method	10, 18, 21	2.0491
Full enumeration	10, 20, 23	2.0569

The results obtained using three different optimization approaches, namely EI, the proposed method and the full enumeration have been shown in Table 1. From this table we can conclude that both approximate methods found the same local optimum (objective function value = 2.0491), while the full enumeration gave a slightly better global optimum with the objective function value equal to 2.0569. Graphically both solutions have been shown in Figure 4.
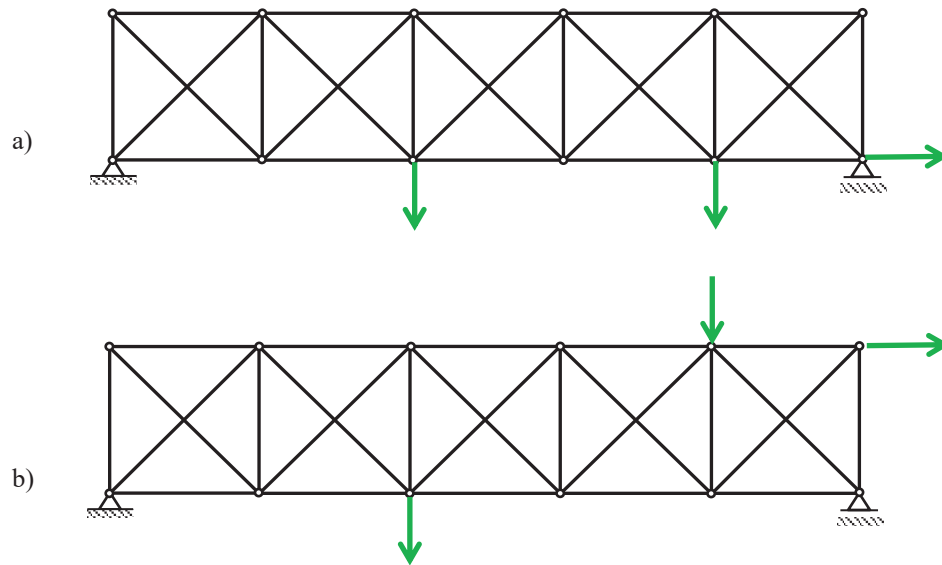
FIGURE 4. Local (a) vs global (b) optimal solution

Example 2: Two-story frame structure

The second example concerns a two-story steel structure consisting of two vertical columns and two horizontal beams assembled using pin connections. The structure and its dimensions are shown in Fig. 5. It has been assumed that the lengths of both horizontal beams is equal to $l = 2$. The properties and dimensions of the structure are listed in Table 1.
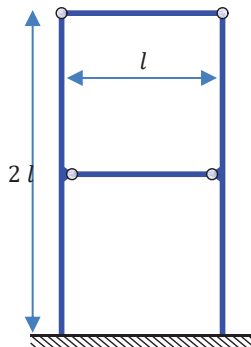

TABLE 2. Properties of the considered structure

Quantity	Symbol	Value
Young modulus (steel)	E [Pa]	$210 \cdot 10^9$
Material density (steel)	ρ [kg/m³]	7860
length	l [m]	2
Cross section area (square)	A [mm²]	$0.01 \times 0.01 = 10^{-4}$

FIGURE 5. Frame structure

The structure has been discretized with the aid of the finite elements method. A mesh of equidistant nodes has been imposed with the distance between nodes equal to $l/3$. The vertical beams have 6 finite elements (FE) and the horizontal beam has 3 FE based on the Euler-Bernoulli beam theory. The cubic shape functions have been assumed. The first four mode shapes and the corresponding natural frequencies are shown in Fig. 6. It is visible that third and fourth modes are orthogonal to the remaining other ones, but first and second are not.
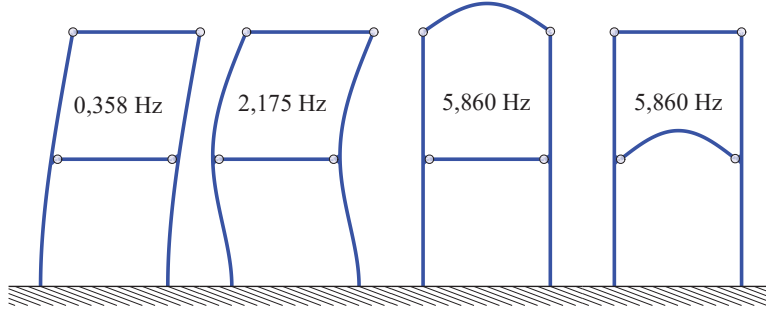
FIGURE 6. Mode shapes and natural frequencies of modes selected for identification

In this example, the execution of iterations is stopped when the condition below is satisfied.

$$\sum_{i=1}^{N_\rho} \left| \rho_i^{(j)} - \rho_i^{(j-1)} \right| < N_m \kappa_{\text{tol}}. \tag{17}$$

Here j is the number of iteration and i is the index of element of $\boldsymbol{\rho}$, while κ_{tol} is an arbitrarily imposed value. From the fact that the matrix $\mathbf{E}_{\mathcal{F}}^{\mathcal{C}}$ from eq. (17) is idempotent and has the same trace for each iteration equal to N_m, it follows that all elements of $\boldsymbol{\rho}$ are always smaller than 1. This is the reason why the elements of the sum in eq. (17) are not normalized by any norm of $\boldsymbol{\rho}$. Here, $\kappa_{\text{tol}} = 10^{-5}$. Value of κ_{tol} is not so important because the algorithm chooses sensor locations related to these values ρ_i that are significantly greater than the remaining ones. In this case DOFs for which $\rho_i > 0.5$ are chosen for sensor placement.

The obtained results are shown in Fig. 7. The set of candidate sensor locations has been limited only to the translational DOFs. As it can be seen in Fig. 7a-b), the condition (17) was satisfied after eight iterations and the calculations were stopped. Figure 7a) shows that the determinant of the Fisher information matrix is not monotonically decreasing like in the Effective Independence method, but initially decreases to eventually increase at the final iterations. The reason of this phenomenon is visible in Fig. 7b). The matrix $\boldsymbol{\Phi}_C$ initially – in the first iteration – has all rows multiplied by ones, in the second iteration the rows of the matrix $\boldsymbol{\Phi}_C$ are multiplied by the elements ρ_i from the first iteration where only one element had a significant value. Thus, the determinant of the matrix $\boldsymbol{\Phi}_C^{\text{T}}\boldsymbol{\Phi}_C$ decreased. In further iterations, the participation of DOFs with the largest contribution to linear independence is gained, hence the determinant of the matrix $\boldsymbol{\Phi}_C^{\text{T}}\boldsymbol{\Phi}_C$ monotonically increases.

One can see that for this special symmetric case, the candidate DOFs 11-14 have the same participation in the linear independence. It is because they are related to the DOFs in which the same displacements appear for modes 3 and 4, see the final result in Fig. 7c). Six DOFs are selected instead of 4 DOFs because of the condition that each DOF with $\rho_i > 0.5$ is to be selected. The algorithm cannot maximize their participation at the expense of other ones. This problem can be avoided by a small disturbance of the initial value of the sensor density vector $\boldsymbol{\rho}$. Such a case is shown in Fig. 8. The elements $\rho_{12}^{(1)}$ and $\rho_{14}^{(1)}$ have been multiplied by 1.1, see Fig 8b). After such an operation, the equilibrium in participation of DOFs 11-14 is disturbed and the contribution of the candidate locations no. 12 and 14 can be maximized at the expense of the others. The final result is shown in Fig. 8c). As it was mentioned, the number of the selected DOFs is finally equal to the number of the modes to be monitored.
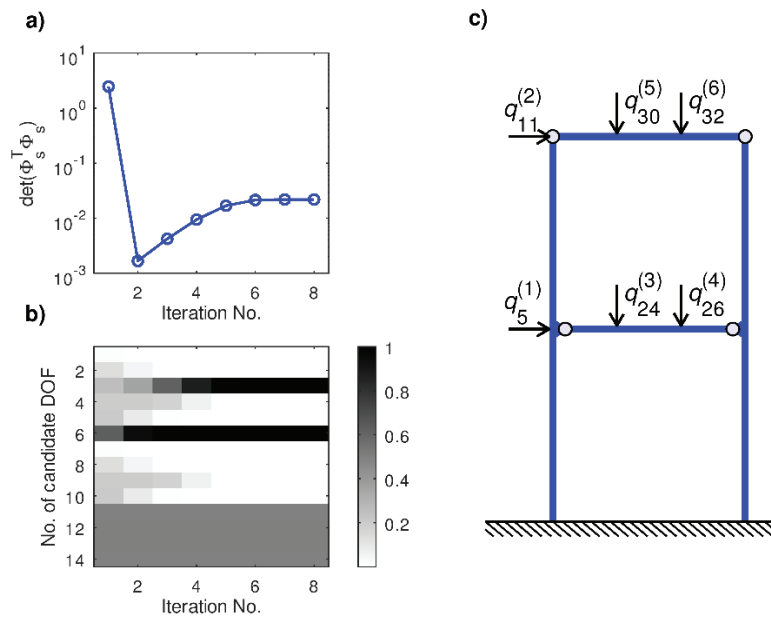
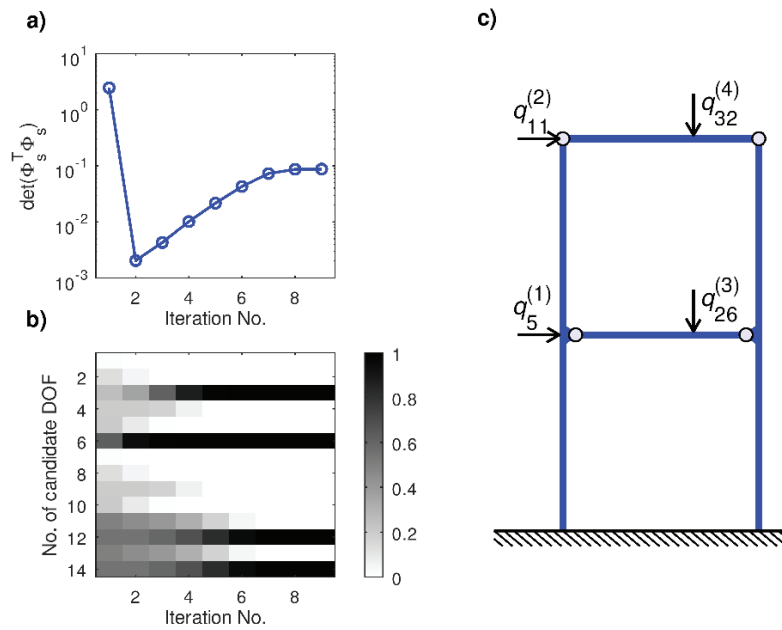**FIGURE 7.** Results given by topology optimization based method: a) values of determinant of the Fisher information matrix for each iteration, b) values of the elements of $\boldsymbol{\rho}$, c) resulting sensor locations

FIGURE 8. Results given by topology optimization based method with initially disturbed $\boldsymbol{\rho}$: a) values of determinant of the Fisher information matrix for each iteration, b) values of the elements of $\boldsymbol{\rho}$, c) resulting sensor locations

CONCLUSIONS

The paper can be summarized with the following most important aspects:
- An efficient method for a sensor network deployment over civil engineering structures was presented. The proposed approach is based on an analogy between the sensor placement and the topology optimization problems.
- A sensor density function has been introduced, which allows the optimal solution to be approached in an iterative way instead of the sequential removal of individual least significant degrees of freedom.
- The effectiveness of the proposed methodology has been demonstrated numerically using two case studies: a simple 5-bay truss bridge and a two-story frame structure.

In future work, an extension of the approach to the problem of optimum actuator placement will be studied, including local and modular control [17,18]. Moreover, formulations specific to substructural monitoring [19], as well as specializations to local monitoring of modular structures [20] and wide-span roofing structures [21] will be investigated and developed.

ACKNOWLEDGMENT

REFERENCES

1. Ou, J., Li, H., *Structural health monitoring in mainland China: Review and future trends*, Structural Health Monitoring **9**(3), 219-231 (2010).
2. An Y., Chatzi E., Sim S., Laflamme S., Błachowski B., Ou J., *Recent progress and future trends on damage identification methods for bridge structures*, Structural Control and Health Monitoring **e2416**, 1-30 (2019).
3. Błachowski B., An Y., Spencer Jr. B.F., Ou J., (2017). *Axial strain accelerations approach for damage localization in statically determinate truss structures*, Computer-Aided Civil and Infrastructure Engineering **32**(4), 304-318 (2017).
4. Pnevmatikos N.G., Błachowski B., Hatzigeorgiou G.D., Świercz A., *Wavelet analysis based damage localization in steel frames with bolted connections*, Smart Structures and Systems**18**(6), 1189-1202 (2016).
5. Hou J., Jankowski Ł., Ou J., *Frequency-domain substructure isolation for local damage*, Advances in Structural Engineering **18**, 137-154 (2015).
6. Błachowski B., *Modal sensitivity based sensor placement for damage identification under sparsity constraint*, Periodica Polytechnica Civil Engineering **63**(2), 432-445 (2019).
7. Hou J., An Y., Wang S., Wang Z., Jankowski Ł., Ou J., *Structural Damage Localization and Quantification Based on Additional Virtual Masses and Bayesian Theory*, Journal of Engineering Mechanics **144**(10), 04018097 (2018).
8. Błachowski B., Świercz A., Jankowski Ł., *Virtual Distortion Method based optimal sensor placement for damage identification*, ISMA 2018 / USD 2018, International Conference on Noise and Vibration Engineering / International Conference on Uncertainty in Structural Dynamics, 2018-09-17/09-19, Leuven (BE), pp.3815-3824 (2018).
9. Kammer D.C. *Sensor placement for on-orbit modal identification and correlation of large space structures*, Journal of Guidance, Control, and Dynamics **14**(2), 251-259 (1991).
10. Bruggi M., Mariani S. *Optimization of sensor placement to detect damage in flexible plates*, Engineering Optimization **45**(6), 659-676 (2013).
11. Tauzowski P., Błachowski B., Lógó J., *Functor-oriented topology optimization of elasto-plastic structures*, Advances in Engineering Software **135**, 102690 (2019).
12. Błachowski B., Tauzowski P., Świercz A., Jankowski Ł., *Topology optimization approach for dense sensor network distribution over large bridge structures*, SMART 2019, 9th ECCOMAS Thematic Conference on Smart Structures and Materials, 2019-07-08/07-11, Paris, France, pp.284-290 (2019).
13. Stephan C. *Sensor placement for modal identification*, Mechanical Systems and Signal Processing **27**, 461-470 (2012).

14. Chepuri S.P., Leus G. Sensor selection for estimation, filtering, and detection, 2014 International Conference on Signal Processing and Communications (SPCOM), Bangalore, India, 22-25 July 2014.
15. Papadimitriou C., Beck J. L., Au S.-K. *Entropy-Based Optimal Sensor Location for Structural Model Updating*. Journal of Vibration and Control **6**(5), 781–800 (2000).
16. Poston W.L., Tolson R.H. *Maximizing the determinant of the information matrix with the effective independence method*, Journal of Guidance, Control, and Dynamics **15**(6), 1513-1514 (1992).
17. Pisarski D., *Decentralized stabilization of semi-active vibrating structures*, Mechanical Systems and Signal Processing **100**, 694-705 (2018).
18. Popławski B., Mikułowski G., Mróz A., Jankowski Ł., *Decentralized semi-active damping of free structural vibrations by means of structural nodes with an on/off ability to transmit moments*, Mechanical Systems and Signal Processing **100**, 926-939 (2018).
19. Hou J., Jankowski Ł., Ou J., *An online substructure identification method for local structural health monitoring*, Smart Materials and Structures **22**(9), 095017 (2013).
20. Zawidzki M., Jankowski Ł., *Multiobjective optimization of modular structures: Weight versus geometric versatility in a Truss-Z system*, Computer-Aided Civil and Infrastructure Engineering **34**(11), 1026-1040 (2019).
21. W. Kaminski, K. Makowska, M. Miskiewicz, J. Szulwic, K. Wilde, *System of monitoring of the Forest Opera in Sopot structure and roofing*, 15th Int'l Multidisciplinary Scientific GeoConference (SGEM) **2**(2), 471–482 (2015).